JCTC Journal of Chemical Theory and Computation

Theoretical Study of the Structure and Electronic Properties of $Si_3O_n^-$ and $Si_6O_n^-$ ($n = 1-6$) Clusters. Fragmentation and Formation Patterns

William Tiznado,*,† Ofelia B. Oña,*,‡ María C. Caputo,‡ Marta B. Ferraro,‡ and Patricio Fuentealba§

Departamento de Ciencias Químicas, Facultad de Ecología y Recursos Naturales, Universidad Andres Bello, Av. República 275, Santiago-Chile, Departamento de Física, Facultad de Ciencias Exactas y Naturales, Universidad de Buenos Aires, Ciudad Universitaria - Pab. I., Argentina, and Departamento de Física, Universidad de Chile, Las Palmeras 3425, Santiago-Chile

Received May 12, 2009

Abstract: A theoretical study of two series of small clusters, $Si_3O_n^-$ and $Si_6O_n^-$ ($n = 1-6$), has been carried out. The minimum energy structures were produced adding an electron to neutral species followed by relaxation at the B3LYP-6-311G(2d) level. The vertical ionization energies (VIEs) were computed using the electron propagator theory (EPT) in two approximations, Unrestricted Outer Valence Green Functions (UOVGF) and partial third-order approximation (P3). In the series $Si_3O_n^-$ the theoretical VIEs of the minimum energy structures agree well with experimental data. For the second series there are not experimental VIEs, and the theoretical results are predictions. The performance of EPT methodologies in conjunction with all-electron or pseudopotentials (PP) calculations is analyzed. The conjunction of P3 and PP approximation proves to be the most efficient and economical methodology to calculate the VIEs of small anionic silicon oxide clusters. In the series $Si_6O_n^-$ different channels of fragmentation have been calculated. The results suggest that the fragments do not have drastic geometric changes and the anionic fragment corresponds to the atoms where the spin density of the initial large cluster is localized. The Fukui function calculated over selected optimized fragments predicts adequately the interaction between them to form large stable clusters.

I. Introduction

In the past years it has been recognized that complex molecules and atomic clusters (ACs) often possess unique properties, which make them interesting objects of research. The unique properties of ACs are intimately related to its geometric and electronic structure. Therefore, a deep understanding of these properties can be essential for various practical applications including the design and formation of new nanostructures as well as the understanding of fundamental issues, such as functioning of quantum and thermodynamic laws (for a review, see refs1−5). The understanding of the principles of assembly and functioning of complex systems like nanoclusters is an open research field, and there is a large number of experimental and theoretical works that approach these problems from different perspectives.[1−5] Even though experimentally accessible quantities are often highly sensitive to cluster structures, there is not a general experimental method for determining such cluster structures. Therefore, detailed theoretical analysis in conjunction with the experimental results is necessary to determine them. In this context, photoelectron spectroscopy (PES) combined with theoretical calculations is one of the most powerful techniques to assign the geometric and electronic structures of clusters. The photoelectron spectra provide information

* Corresponding author E-mail: wtiznado@unab.cl (W.T.), ofelia@df.uba.ar (O.B.O.).
† Universidad Andres Bello.
‡ Universidad de Buenos Aires.
§ Universidad de Chile.

10.1021/ct900320r CCC: $40.75
Published on Web 07/31/2009

about the vertical ionization energies (VIEs) which are directly related to the electronic structure of the system and consequently with its geometric structure, which is generally the global minimum on the corresponding potential energy surfaces. Once the minimum energy structures have been identified, the VIEs can be theoretically calculated and compared with the experimental available data. In the past, this was performed by molecular orbital calculations (MO) and Koopmans' theorem, where the ionization energy is approximated as the negative of the one-electron MO energy.[6] Both correlated and uncorrelated orbital energies respectively based on density functional and Hartree−Fock methods may produce large errors in determining ionization energies and in some cases even give an erroneous ordering of the final electronic states[7−9]

A quasiparticle approximation in electron propagator theory (EPT) is a good methodology to determine vertical ionization energies which are comparable to experimental data. The most used approximation of EPT, known as the outer valence Green Function method, was developed by Cederbaum and co-workers for closed shell systems (ROVGF)[8,9] and by Ortiz and co-workers for open shell systems (UOVGF).[10−12] An efficient approximation to them, the partial third-order approximation, P3, was also developed by Ortiz et al.[13,14]

Silica is one of the most abundant materials on earth.[15] Its nanoparticles are an interesting object of study because of their importance in technological applications such as microelectronics, optics, glass manufacture, catalysis support, and fiber-optic communications.[16,17] Recently, it has been experimentally proved that silicon oxide clusters have a fundamental role in the growth of silicon nanowires.[18] In this context, the study of small clusters based on silicon and oxygen atoms is an interesting research field which is supported by a large number of experimental and theoretical publications.[19−30]

The present work focuses on applying different theoretical methodologies in the study of two sets of small anionic silicon oxide clusters, $Si_3O_n^-$ and $Si_6O_n^-$ ($n = 1-6$). These clusters have been chosen because they involve two series of oxidized silicon clusters where, as the number of oxygen atoms increases, they evolve from silicon rich clusters to oxygen rich clusters for the first set and to 1:1 (silicon and oxygen relation) clusters for the second set. For the series $Si_3O_n^-$, experimentally well resolved photoelectron spectra[18] will be used to evaluate the capability of EPT based methodologies, UOVGF,[10−12] and partial third-order approximation (P3)[13,14] to yield accurate results. For the series $Si_6O_n^-$ a theoretical study[30] about the global minimum will be also used to compare with our results.

In section III, the results are reported in a sequential way. First, we verified the minimum energy structures as reported in previous studies.[30] Then, we calculated the VIEs of the more stable isomers by means of the EPT methodologies. Theoretical assignment of the experimental photoelectron spectra was only possible for the first set of clusters, whereas in the second set the calculations are only predictive due to the absence of experimental data to compare with. In the second series of clusters ($Si_6O_n^-$) the minimum energy fragmentation channels were evaluated. Finally, we studied the formation of the largest clusters ($Si_6O_n^-$) from the interaction of the stabilized fragments. As predictor of the most probable interacting region we used condensed in atoms Fukui functions.

II. Methodologies

A. Anionic Structures. In order to determine the most stable isomers of $Si_3O_n^-$ and $Si_6O_n^-$ we employed the neutral structures taken from refs 20 and 29. For both sets of clusters we produced the anionic states adding one electron to each stable neutral isomer followed by B3LYP[31]/6-311G(2d)[32,33] relaxation to their corresponding local anionic minima.

B. Electron Propagator. Two approximated electron propagator methods have been applied to the VIEs predictions: the unrestricted outer valence Green's function (UOVGF) approximation[8,9,34] and the partial third-order approximation (P3)[13,14] which has clear computational advantages over UOVGF methods. They are used in combination with all-electron and pseudopotential (PP) calculations.

Whereas all-electron calculations employed the 6-311G-(2d)[32,33] basis sets, the Stuttgart pseudopotential for Si and O was combined with its corresponding basis functions.[35] Because the latter basis set does not contain diffuse and polarization functions, it was augmented with the most diffuse *s* and *p* functions and two contracted *d*-polarization functions of Sadlej's basis set.[36] This augmented basis set has already proven to be accurate enough for the calculation of the dipole polarizabilities of neutral silicon clusters and for VIEs calculations of small anionic silicon clusters.[37]

C. Local Reactivity Descriptor. The local reactivity descriptor used in this work is the Fukui function which was calculated by the finite difference approximation using atomic charges as proposed by Yang and Mortier,[38] $f_k^+ = q_k(m+1) - q_k(m)$ and $f_k^- = q_k(m) - q_k(m-1)$, where f_k^+ and f_k^- are the acceptor (electrophilic) and donor (nucleophilic) Fukui functions condensed at atom k respectively, m is the total electron number of the studied system, and $q_k(m)$, $q_k(m+1)$, and $q_k(m-1)$ are the atomic charges evaluated at the atom k in the geometry of the studied system by adding 0, 1, and −1 electrons, respectively. The atomic charges were obtained from two different methods, natural population analisys (NPA)[39−41] and ChelpG[42] (CHG). The last one was evaluated to include information about the possible electrostatic effects on the interactions.

All the calculations were done using the GAUSSIAN 03 package of programs.[43] The pictures of the structures and spin density isosurfaces were performed with the Molekel 4.3 visualization program.[44]

III. Results and Discussion

A. Search of the Minimum Energy Structures. *$Si_3O_n^-$ Clusters.* It was found that in all cases the previously reported structures[20] for the neutral clusters are the most stable ones. In the case of the $Si_3O_3^-$ cluster the planar C_s structure (see Figure 1-SI) was found as a local minimum isomer which is 0.09 eV above the global minimum structure

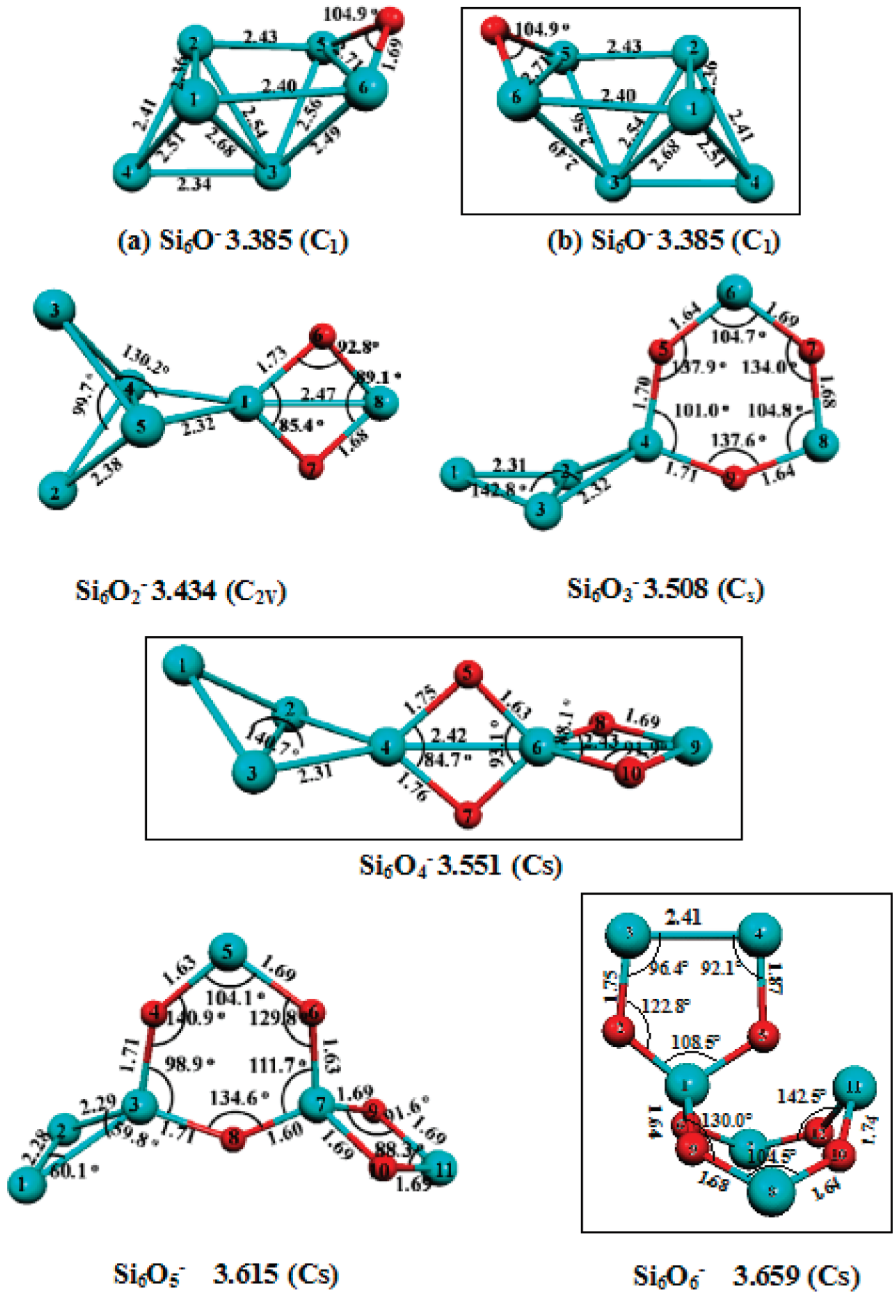

Figure 1. Structures of the ground state for anionic $Si_6O_n^-$ ($n = 1-6$) clusters obtained by adding one electron to these reported in ref 29 and followed by B3LYP/6-311G(2d) local optimization. Absolute binding energies per atom (BE/atom) are in eV, based on a Si atomic energy of −7847.211 eV, an anionic Si atomic energy −7847.193, and O atomic energy of −2038.703 eV ($BE = E(Si_6O_n^-) - 5E(Si) - E(Si^-) - nE(O_2/2)$). The new minimal structures found in this work are enclosed in frames.

at the MP2/cc-pVTZ[45,46] level, including the zero point energy correction in the energy calculations.

$Si_6O_n^-$ Clusters. After exploring different isomers we found some new structures with respect to those previously reported by Zang et al.[30] The clusters and the principal structural data are reported in Figure 1. Two isoenergetic Si_6O^- clusters were found, denoted as (a) and (b) in the figure, which are not superposable mirror structures of the same isomer. Zang et al.[30] only reported the Si_6O^-(a) ground state. Within our scheme the new $Si_6O_4^-$ and $Si_6O_6^-$ structures with C_s symmetry are the global minimum. They are 0.13 and 0.12 eV more stable (at the B3LYP/6-311G(2d) level) than the other isomers, respectively.

Calculation of the VIEs Using UOVGF and P3 Methodologies. Tables 1 and 2 present results of the theoretical calculation of the final state orbital assignments, VIEs, and pole strengths (in parentheses) of the $Si_3O_n^-$ and $Si_6O_n^-$ ($n = 1-6$) clusters in comparison with other theoretical predictions and experimental values. The expectation values of $\langle S^2 \rangle$ (total spin) for the reference Slater determinant are less than 0.8 (see Table 1-S), and the pole strengths are greater than 0.85 in all the studied systems. These results validate the quality of the electron propagator methods used in the present work to predict the VIEs.

$Si_3O_n^-$ Clusters. There is a good agreement between UOVGF and P3 results. In the all-electron results the higher

Table 1. Comparison of Experimental and Pseudopotential Calculations of Vertical Electron Detachment Energies (VEDEs) in eV for the $Si_3O_n^-$ ($n = 1-6$) Series[c]

				all-electron		pseudopotential			
system	initial state	final state	orbital	6-311G(2d) UOVGF(p)[a]	P36-311G(2d) (p)[a]	UOVGF(p)[a]	P3(p)[a]	experiment[b]	$\Delta E(E\nu+1\text{-}E\nu)$
		$^3B_2$	$5a_1$	2.67(0.89)	2.68(0.88)	2.91(0.88)	2.79(0.88)	3.1	
Si_3O^-	$^2B_2$	$^1A_2$	$2b_1$	2.41(0.89)	2.50(0.88)	2.62(0.88)	2.59(0.88)	2.6	
		$^3A_2$	$2b_1$	2.25(0.90)	2.34(0.89)	2.46(0.89)	2.43(0.88)	2.5	
		$^1A_1$	$3b_2$	1.58(0.89)	1.65(0.88)	1.79(0.88)	1.73(0.87)	1.96(0.06)	1.87
		$^3B_1$	$5a_1$	4.90(0.89)	4.73(0.89)	5.15(0.88)	4.83(0.89)		
$Si_3O_2^-$	$^2B_1$	$^1A_1$	$2b_1$	1.99(0.91)	1.94(0.91)	2.23(0.90)	2.07(0.90)	2.2	
		$^1B_1$	$6a_1$	1.97(0.89)	1.81(0.89)	2.20(0.88)	1.94(0.89)	2.1	
		$^3B_1$	$6a_1$	1.74(0.89)	1.60(0.89)	1.98(0.88)	1.73(0.88)	2.03(0.06)	1.83
		$^1A''$	$6a''$	4.15(0.87)	3.92(0.87)	4.40(0.86)	4.02(0.86)	4.2	
$Si_3O_3^-$	$^2A'$	$^3A'$	$9a'$	3.79(0.86)	3.62(0.87)	4.0(0.86)	3.68(0.86)	3.9	
		$^3A''$	$6a''$	3.71(0.85)	3.49(0.85)	3.94(0.84)	3.60(0.85)	3.8	
		$^1A'$	$10a'$	1.23(0.91)	1.17(0.91)	1.46(0.90)	1.28(0.91)	1.50(0.10)	1.54
		$^3B_2$	$7a_1$	6.50(0.91)	6.42(0.91)	6.71(0.91)	6.52(0.91)		
$Si_3O_4^-$	$^2B_2$	$^1B_2$	$8a_1$	5.07(0.87)	4.88(0.87)	5.36(0.86)	5.02(0.86)		
		$^3B_2$	$8a_1$	4.32(0.90)	4.11(0.90)	4.59(0.89)	4.27(0.89)	4.4	
		$^1A_1$	$5b_2$	0.98(0.93)	0.88(0.93)	1.21(0.92)	1.03(0.93)	1.055(0.050)	1.07
		$^1A''$	$7a''$	5.87(0.93)	5.48(0.91)	6.38(0.94)	5.66(0.91)		
$Si_3O_5^-$	$^2A'$	$^3A''$	$7a''$	5.76(0.94)	5.34(0.91)	6.25(0.94)	5.51(0.91)		
		$^3A'$	$14a'$	5.67(0.93)	5.29(0.91)	6.20(0.93)	5.51 (091)		
		$^1A'$	$15a'$	3.20(0.93)	3.27(0.92)	3.54(0.93)	3.45(0.92)	3.1(0.1)	3.11
		$^1A''$	$8a''$	6.36(0.93)	5.99(0.91)	6.85(0.94)	6.17(0.91)		
$Si_3O_6^-$	$^2A'$	$^3A''$	7a''	6.24(0.94)	5.85(0.92)	6.72(0.94)	6.02(0.91)		
		$^3A'$	$16a'$	6.15(0.93)	5.80(0.91)	6.68(0.93)	6.02(0.91)		
		$^1A'$	$17a'$	3.73(0.93)	3.85(0.92)	4.07(0.93)	4.03(0.92)	>3.5	3.68

[a] Pole strengths. [b] Anion photoelectron spectra.[20] [c] Theoretical predictions have been calculated with the OVGF approximation of electron propagator theory using the 6-311G(2d) basis set.

Table 2. Pseudopotential Calculations of Vertical Electron Detachment Energies (VEDEs) in eV for the $Si_6O_n^-$ ($n = 1-6$) Series[b]

system	initial state	final state	orbital	all-electron 6-311G(2d) UOVGF (p)[a]	pseudopotential (p)[a]
Si_6O^-	^2A	^3A	$14a$	3.30(0.89)	3.57(0.87)
		^1A	$15a$	3.14(0.89)	3.37(0.87)
		^3A	$15a$	2.99(0.89)	3.22(0.87)
		^1A	$16a$	2.67(0.89)	2.90(0.88)
$Si_6O_2^-$	$^2A_1$	$^1B_2$	$5b_2$	3.55(0.88)	3.57(0.87)
		$^3A_2$	$2a_2$	3.4290.88)	3.55(0.87)
		$^3B_2$	$5b_2$	3.20(0.88)	3.27(0.87)
		$^1A_1$	$9a_1$	3.09(0.89)	3.11(0.88)
$Si_6O_3^-$	$^2A''$	$^3A''$	$15a'$	3.61(0.88)	3.63(0.87)
		$^1A''$	$16a'$	3.49(0.88)	3.53(0.87)
		$^3A''$	$16a'$	3.31(0.88)	3.35(0.87)
		$^1A'$	$6a''$	2.11(0.88)	2.18(0.87)
$Si_6O_4^-$	$^2A''$	$^3A''$	$15a'$	3.80(0.88)	3.83(0.87)
		$^1A''$	$16a'$	3.70(0.88)	3.79(0.87)
		$^3A''$	$16a'$	3.54(0.89)	3.63(0.87)
		$^1A'$	$9a''$	2.38(0.88)	2.48(0.87)
$Si_6O_5^-$	$^2A''$	$^3A''$	$19a'$	3.17(0.89)	3.17(0.88)
		$^1A''$	$18a'$	3.02(0.88)	3.01(0.88)
		$^3A''$	$18a'$	2.82(0.88)	2.79(0.88)
		$^1A'$	$9a''$	2.71(0.88)	2.76(0.87)
$Si_6O_6^-$	$^2A''$	$^3A''$	$18a'$	4.73(0.89)	4.51(0.89)
		$^1A'$	$12a''$	3.21(0.89)	3.17(0.90)
		$^1A''$	$19a'$	3.15(0.91)	3.11(0.89)
		$^3A''$	$19a'$	2.99(0.88)	2.91(0.88)

[a] Pole strengths. [b] Theoretical predictions have been calculated with the UOVGF approximation of electron propagator theory using the 6-311G(2d) basis set.

differences are of the order of 0.4 eV between the two approximations (UOVGF and P3), and in all cases, with the exception of Si_3O^-, the VIEs-UOVGF are higher than their respective P3 values. The pseudopotential (PP) results in both approximations (UOVGF and P3) are higher than the all-electron ones, and they are closer to the experimental values. We compared our theoretical estimations with the high values of each band in the experimental spectra.[20] The UOVGF/PP results reproduce better the experimental values, but in general P3/PP seems to be an adequate methodology in predictions of VIEs. These results could be extrapolated to the study of larger silicon oxides clusters with the most economical methodology tested in this work. The last column of Table 1 shows the results obtained using finite difference

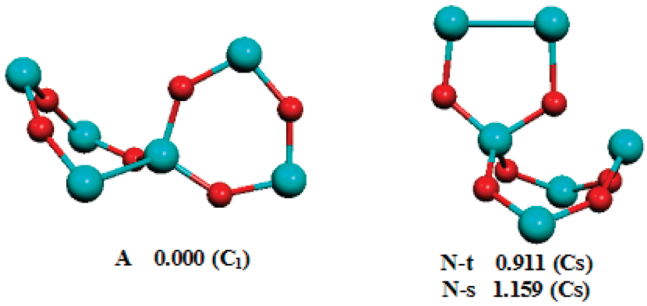

Figure 2. Structures of the most stable neutral Si_6O_6 (A) reported in ref 29 and Si_6O_6 (N) obtained by subtracting one electron to $Si_6O_6^-$ and followed by B3LYP/6-311G(2d) optimization. Singlet spin state is N-s and triplet spin state is N-t. We report the relative energy of each cluster with respect to structure A.

approximations. It means that the vertical ionization energy is calculated as the difference between the anion and the neutral cluster at the geometry of the anion. The values compare very well with the experimental ones and those calculated using EPT (UOVGF and P3) methods. However, in the finite difference approximation one needs to do two calculations and obtains only the first transition.

In Si_3O^-, $Si_3O_3^-$-$Si_3O_6^-$, the first vertical ionization energy calculated by the electron propagator methodologies corresponds to the ejection of the nonpaired electron to yield the corresponding closed shell neutral species. On the contrary, $Si_3O_2^-$ presents a first ionization energy corresponding to the transition toward the triplet state of the neutral cluster. However, the transition to the singlet state is only 0.22 eV higher in energy at the UOVGF/PP level of calculation. This is in agreement with the discussion by Lai-Sheng Wang et al.[20] They used energy differences between the anionic cluster and the singlet and triplet neutral ones (three calculations) for their assignments.

The planar C_s, $Si_3O_3^-$, was found to be closer in energy to the one of minimum energy (Part A of the discussion). In order to evaluate the possible experimental evidence of this cluster, we calculated its VIEs at UOVGF/PP approximation. The calculated VIEs of the most external valence electrons are $\alpha(4a'')$ 1.05 eV, $\beta(12a')$ 4.02 eV, and $\beta(11a')$ 4.63 eV, and the pole strengths values are between 0.85 and 0.91. All the predicted VIEs are in the ranges of the peaks of the Wang's experimental spectra.[20]

$Si_6O_n^-$ Clusters. The VIEs calculated at UOVGF/all-electron and P3/PP levels of theory are reported in Table 2. The results obtained by all-electron and PP calculations show the same systematic trend presented in the $Si_3O_n^-$ clusters, and the P3/PP values are higher than their OVGF/all-electron counterpart.

In the clusters $Si_6O_n^-$ ($n = 1-5$) the first VIEs correspond, from our calculations, to the ejection of the nonpaired electron, giving as a result a closed shell neutral cluster. In the case of the $Si_6O_6^-$ the calculations show that the first ionization gives as a result a neutral cluster in a triplet ground state. In order to verify whether this open shell cluster is the most stable, the geometry was relaxed to the minimum and compared with the neutral structure reported in the literature.[29,30] We optimized the system at the B3LYP/6311 g(2d) level, which is displayed as N-t (N structure-triple spin state) in Figure 2. We display in the same figure the most stable structure for neutral Si_6O_6 (A), which is a singlet. The N-t state is 0.911 eV less stable than isomer A, but 0.248 eV is more stable than N-s, an isomer with the same geometry as N-t but in the singlet state. In Figure 2 all energies are referred as to structure A.

Diffuse functions are not included in the all-electron UOVGF and P3 results, inclusions likely to lead to larger electron binding energies, and, therefore, the pseudopotential calculations which include diffuse functions give closer agreement with the experimental data.

C. Study of the Fragments. *Spin Density Localization.* The spin density isosurfaces show that the spin density is mainly localized over the silicon atoms in the $Si_3O_n^-$ series (Figure 2-SI) and over the silicon rich fragment in the $Si_6O_n^-$ series. In the $Si_3O_5^-$ and $Si_3O_6^-$ clusters the spin density is mainly localized over the terminal silicon atoms and their surrounding oxygen atoms. These Si atoms have a sp^3 like hybridization which gives them an electronegative character. This is in agreement with the high first vertical ionization energy of these clusters. A relation of the spin density localization and the value of the first ionization energy in

Table 3. Fragmentation Energies (FE) and Fragmentation Channels for the Most Stable Anion $Si_6O_n^-$ ($n = 1-6$) Clusters Obtained at the B3LYP/6-311G(2d) Level of Theory

Si_6O_m	$\rightarrow Si_kO_l^-$	$+ Si_{6-k}O_{m-l}$	FE (eV)	Si_6O_{4m}	$\rightarrow Si_kO_l^-$	$+ Si_{6-k}O_{m-l}$	FE (eV)
Si_6O^-	Si_5^-	SiO	1.437	$Si_6O_4^-$	Si_3^-	Si_3O_4	1.989
	Si_4^-	Si_2O	3.369		Si_3O^-	Si_3O_3	2.471
	Si_3^-	Si_3O	3.895		$Si_4O_2^-$	Si_2O_2	3.043
	Si_5	SiO^-	4.067		$Si_3O_3^-$	Si_3O	3.513
	Si_4	Si_2O^-	4.077		$Si_3O_4^-$	Si_3	3.587
$Si_6O_2^-$				$Si_6O_5^-$	Si_2^-	Si_4O_5	2.389
	Si_4^-	Si_2O_2	1.956		$Si_3O_2^-$	Si_3O_3	2.456
	$Si_2O_2^-$	Si_4	3.014		$Si_5O_4^-$	SiO	2.570
	Si_3^-	Si_3O_2	3.383		Si_3O^-	Si_3O_4	2.783
	Si_5^-	SiO_2	3.591		$Si_3O_3^-$	Si_3O_2	3.480
	$Si_3O_2^-$	Si_3	3.843		$Si_4O_4^-$	Si_2O	3.669
$Si_6O_3^-$	Si_3^-	Si_3O_3	1.998	$Si_6O_6^-$	$Si_3O_3^-$	Si_3O_3	2.135
	$Si_5O_2^-$	SiO	2.734		$Si_4O_4^-$	Si_2O_2	2.620
	Si_4^-	Si_2O_3	3.172		$Si_3O_2^-$	Si_3O_4	2.652
	$Si_3O_3^-$	Si_3	3.482		$Si_2O_2^-$	Si_4O_4	3.120
	Si_3O^-	Si_3O_2	4.021		$Si_3O_4^-$	Si_3O_2	3.789

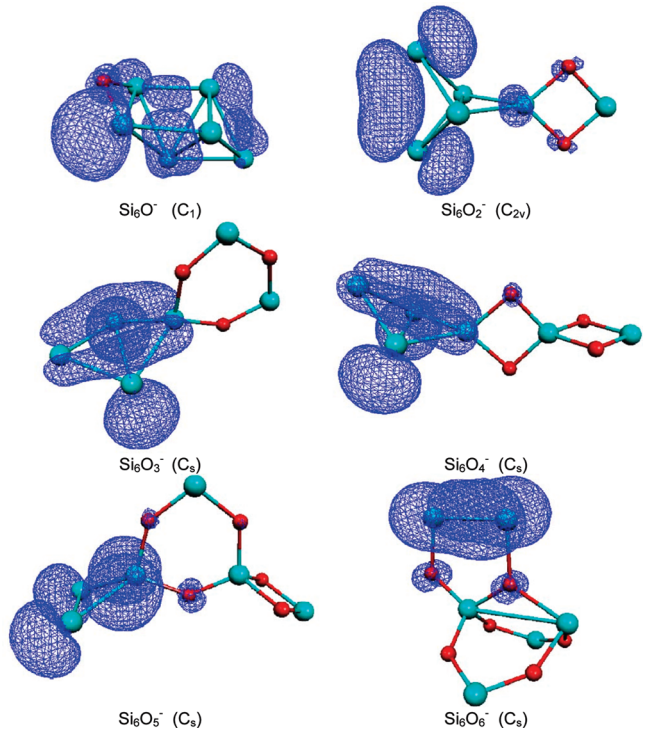

Figure 3. Spin density of the ground state for anionic $Si_6O_n^-$ ($n = 1-6$) clusters obtained at the B3LYP/6-311G(2d) level of theory.

the $Si_6O_n^-$ series is not obvious because the spin density is more delocalized over all the silicon rich fragment.

Fragmentation Energies. We have studied some fragmentation channels for the most stable structures of the $Si_6O_n^-$ ($n = 1-6$) clusters. The energy associated with each fragmentation channel $Si_6O_n^- \rightarrow Si_kO_l^- + Si_{6-k}O_{n-l}$ is defined as $FE = E(Si_kO_l^-) + E(Si_{6-k}O_{n-l}) - E(Si_6O_n^-)$, and the results are shown in Table 3. Basically, we focused our analysis in those fragmentation channels where one anionic and one neutral fragment are produced. We reported only five lower-energy fragmentation channels. It is interesting to remark that the more energetically favored channels are those where the anionic fragment coincides with the spin density localization in the unfragmented cluster (see Figure 3 and Table 3). Then, energetically favored fragmentation products contain the anionic Si_3^-, Si_4^-, Si_5^-, $Si_3O_2^-$, and $Si_3O_3^-$ and the neutral SiO, Si_2O_2, Si_3O_2, Si_3O_3, Si_3O_4, and Si_4O_4 clusters.

For Si_6O^-, the most favorable fragmentation channel is $Si_6O^- \rightarrow Si_5^- + SiO$. This channel presents similarities with fragmentation of Si_nO ($n = 5-10$) clusters where $Si_nO \rightarrow Si_n + SiO$ is the most favorable fragment pathway as discussed by H. Wang et al.[47]

$Si_6O_2^-$ presents $Si_6O_2^- \rightarrow Si_4^- + Si_2O_2$ as the most favorable fragmentation channel. So, we could say that $Si_6O_2^-$ is formed by Si_4^- and Si_2O_2, where the pure silicon cluster is an approximation to the ground state of the anionic Si_4^- cluster. Therefore, the extra electron is not localized on the Si_2O_2 fragment in agreement with the localization of the spin density (Figure 3).

The most favorable fragmentation channel for $Si_6O_3^-$ is $Si_6O_3^- \rightarrow Si_3^- + Si_3O_3$, and its spin density shows localization on the Si_3^- fragment. Therefore, the ground state of $Si_6O_3^-$ can be seen as formed by the fragments Si_3^- and Si_3O_3. The second fragmentation channel, with a FE 0.736 eV higher than the first one, is $Si_6O_3^- \rightarrow Si_5O_2^- + SiO$ where the SiO molecule is neutral again.

The most favorable fragmentation channel for $Si_6O_4^-$ contains Si_3^- and Si_3O_4 as products. $Si_6O_4^- \rightarrow Si_3O^- + Si_3O_3$ is 0.482 eV higher than the minimum FE, 1.989 eV.

The most favorable fragmentation channel for $Si_6O_5^-$ is $Si_6O_5^- \rightarrow Si_2^- + Si_4O_5$, although $Si_6O_5^- \rightarrow Si_3O_2^- + Si_3O_3$ and $Si_6O_5^- \rightarrow Si_5O_4^- + SiO$ are only 0.076 and 0.190 eV higher than the minimum FE, 2.380 eV.

Finally, in the case of $Si_6O_6^-$ the most favorable fragmentation channel is $Si_6O_6^- \rightarrow Si_3O_3^- + Si_3O_3$, but there are two fragment pathways with FE close to the minimum FE, 2.135 eV. $Si_6O_6^- \rightarrow Si_4O_4^- + Si_2O_2$ has a FE higher, by 0.032 eV, with respect to the fragmentation channel $Si_6O_6^- \rightarrow Si_3O_2^- + Si_3O_4$, 2.620 eV.

In most cases SiO, Si_2O_2, and Si_3O_3 appear as a product. It seems that Si_2O_2, Si_3O_3, and SiO preserve their stability within the anionic systems. Note that there is a relation between the most favorable fragment channel and the localization of the spin density. The anionic fragments are silicon-rich clusters. This behavior is similar in the spin density.

In Table 4 the principal vibrational modes for $Si_6O_n^-$ structures are reported. In the first column, the principal vibrational frequencies are shown. We tried to identify these modes with the corresponding vibrational modes of the fragmentation byproducts. Therefore, we present vibration modes of the fragment products measured by Anderson et al.[19] and calculated at the B3LYP/6-311G(2d) level of theory. Note that the vibrational modes of $Si_6O_2^-$, $Si_6O_3^-$, and $Si_6O_5^-$ are close to the vibrational modes of the fragment product of the most favorable fragmentation channel. $Si_6O_4^-$ contains the vibrational mode of Si_2O_2, and the fragmentation channel with this product is higher by 1.053 eV than the minimum

Table 4. Vibration Frequencies for $Si_6O_n^-$ ($n = 1-6$) Clusters and Some of Their Fragmentation Products[e]

Si_6O_m[a]	vibration frequencies principal modes		fragmentation product[b]
Si_6O^-	730.7		
$Si_6O_2^-$	750	766.6[c]	*(Si_2O_2)*
		766.3[d]	
$Si_6O_3^-$	*965.7*	957.6[c]	(Si_3O_3)
		972.6[d]	
$Si_6O_4^-$	*726.0*	766.6[c]	*(Si_2O_2)*
		766.3[d]	
	1017.7	1008.4[c]	*(SiO_2)*
$Si_6O_5^-$	*1044.5*	1260.8[c]	*(SiO)*
		1223.9[d]	
	984.4	957.6[c]	*(Si_3O_3)*
		972.6[d]	
	831.7	801.3[c]	*(Si_2O_2)*
		804.7[d]	
$Si_6O_6^-$	*974.9*	845.8[c]	*($Si_4O_4^-$)*
	996.2	1008.4[c]	*(SiO_2)*

[a] This work. [b] Indicated in $Si_6O_m^- \rightarrow Si_kO_l^- + Si_{6-k}O_{m-l}$. [c] The geometries were optimized at the B3LYP/6-311G(2d) level of theory. [d] Vibration frequencies from the mass spectra reported in ref 19. [e] We report the frequencies for principal modes of the most stable isomer of each cluster.

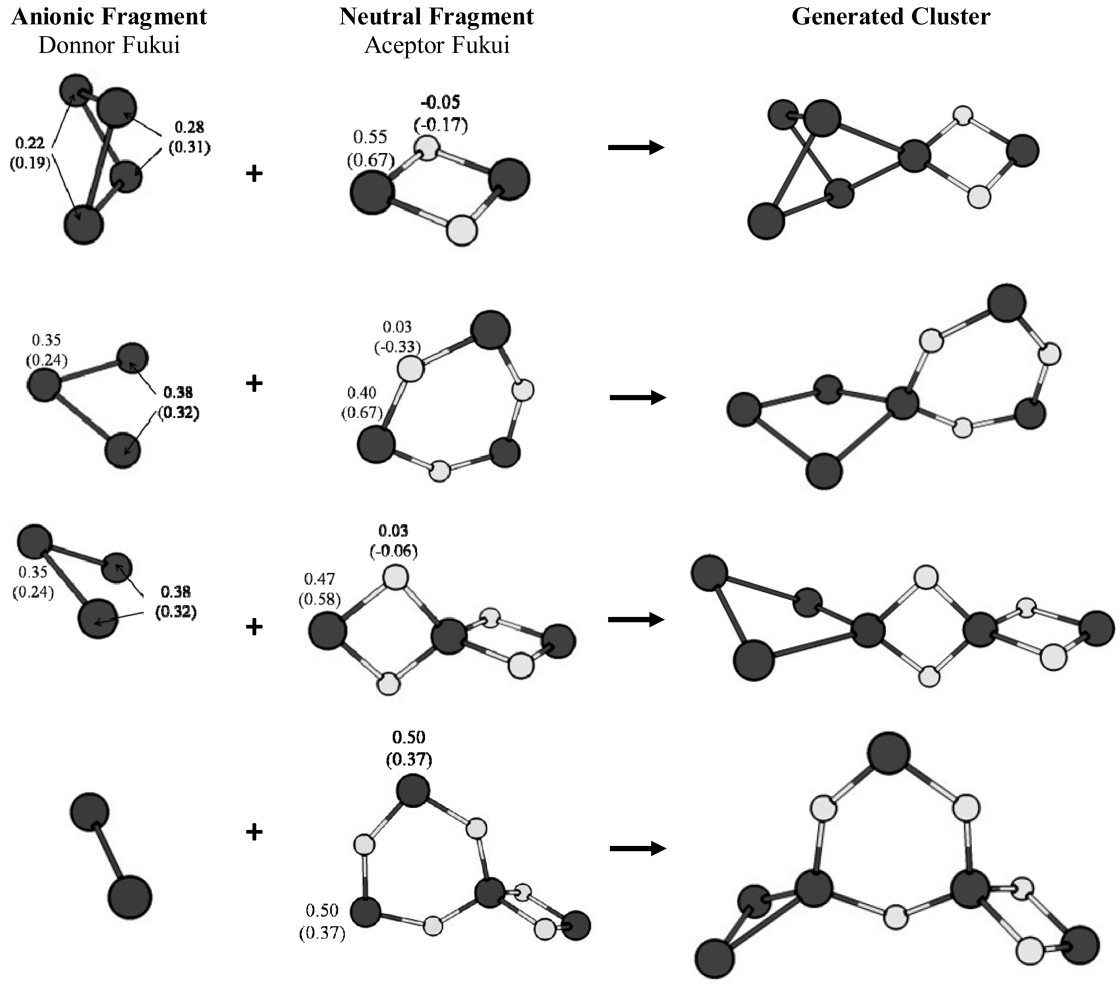

Figure 4. Reactions of formations of large anionic clusters from optimized fragments. Calculated atomic Fukui functions over the fragments, using NPA and CHG charges (in parentheses).

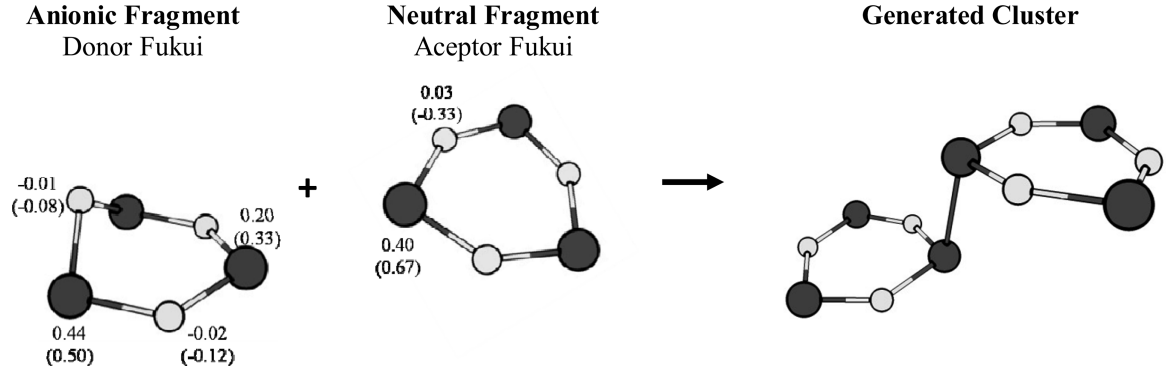

Figure 5. Reactions of formation of $Si_6O_6^-$ D_{2h} clusters from optimized fragments. Calculated atomic Fukui functions over the fragments, using NPA and CHG charges (in parentheses).

FE, 1.989 eV. $Si_6O_6^-$ has one vibrational mode corresponding to that of the $Si_4O_4^-$ product. The fragmentation channel involving this product is only 0.485 eV higher than the minimum FE, 2.134 eV. In most of the cases, the vibrational modes of the fragments present in the most favorable fragmentation channel are similar to the principal modes of the studied anionic systems.

Building Large Clusters from the Small Stabilized Fragments. Previously we have analyzed the fragmentation patterns of $Si_6O_n^-$ series and obtained some characteristic fragments which after energy relaxation are stables structures. In the experimental conditions it is possible that fragmentation and formation are competitive reactions, and thermodynamically the formation reactions in these systems are favored (energy channel analysis). We include an analysis based on the Fukui function with the aim to rationalize the clusters formation from smaller ones, which allows us to identify the most favorable site to interact and therefore to predict the formation of larger systems.

A set of the most characteristic fragments was optimized and calculated the respective donor, f_r^-, and acceptor, f_r^+, condensed Fukui functions, where the donor fragments are

those with negative charge and the acceptor are the neutral ones. The results are shown in the first two columns of Figure 4. Following the selective reactivity criteria the fragments should react in those regions where the respective Fukui values are maxima. The relaxed structures are shown in the last column of Figure 4, and one can see that the structures for $Si_6O_n^-$ ($n = 1-5$) could be obtained by reaction between two small stable fragments.

A formation picture based on Fukui function analysis of the $Si_6O_6^-$ cluster is more complicated. The fragments $Si_3O_3^-$ and Si_3O_3 are the most energetically favored fragments of this cluster (Table 2). The reaction of these two small clusters produce a stable $Si_6O_6^-$ isomer with D_{2h} symmetry (Figure 4) which is 0.52 eV less stable with respect to the minimum energy. The apparent limitation of the Fukui function in predicting the more stable product was discussed by Tiznado et al.[48] in the reaction of hydrogen atoms with silicon clusters. The more stable reactant did not always generate the more stable product.

A complementary analysis of the relaxation pathways which connects different structural isomers with the global minimum structure will be necessary to complement the information obtained from the Fukui function analysis.

IV. Conclusions

A theoretical study of the two series of small clusters $Si_3O_n^-$ and $Si_6O_n^-$ ($n = 1-6$) has been carried out. It has been found that planar $Si_3O_3^-$ D_{3h} cluster is closer in energy to the minimum energy isomer, and its calculated VIEs agree with the experimental ones obtained from the PES experiments. Hence, the experimental presence of this isomer should be not discarded.

Two not previously reported minimum energy isomers were found, $Si_6O_4^-$ and $Si_6O_6^-$. The most stable isomer Si_6O^- is present as two isoenergetic not superimposable mirror images. The P3 methodology in conjunction with the use of effective core pseudopotentials proves to be adequate to calculate the VIEs in small anionic silicon oxides clusters. This was verified comparing to the more complete UOVGF approximation and to the experimental values in $Si_3O_n^-$ ($n = 1-6$) clusters. The propagator methodology establishes that the triplet state of the Si_6O_6 cluster is more stable than the closed shell configuration obtained from the ionization of the most stable anionic cluster. However, the minimum energy structure of the neutral cluster is closed shell. The studied fragmentation channels determine the most stable fragments. In all cases the anionic fragments agree with the localization of the spin density in the large cluster. The spin density is mainly localized on the silicon rich fragment.

The donor and acceptor Fukui functions predict the best interactions between a small anionic silicon cluster and a small neutral silicon oxide cluster to form $Si_6O_n^-$ ($n = 2-5$) global minimum structures, but the $Si_6O_6^-$, obtained from the Fukui function predictions, is not the minimum energy one. A detailed study of the energy pathways which connects different isomers will be necessary to complement the predictions obtained from the Fukui function.

Acknowledgments. Financial support for this work from the University of Buenos Aires, and the Argentinian CONICET, is sincerely acknowledged. W. Tiznado acknowledged Fondecyt's support for its post doctoral fellowship, project No. 3080042, and Dr. P. Jaque for interesting discussions. Part of this work has also been supported by Fondecyt Grants 1080184.

Supporting Information Available: Cartesian coordinates and absolute energies of $Si_3O_3^-$ clusters. Spin density of the ground state for anionic $Si_3O_n^-$ ($n = 1-6$) clusters. Hartree−Fock expectation value of the total spin, $<S^2>$, for $Si_3O_n^-$ and $Si_6O_n^-$ clusters ($n = 1-6$). This material is available free of charge via the Internet at http://pubs.acs.org.

References

(1) Connerade, J. P.; Solov'yov, A. V.; Greiner, W. *Europhysics News* **2002**, *33*, 200.

(2) *NATO Advanced Study Institute, Session LXXIII, Summer School "Atomic Clusters and Nanoparticles"*; Guet, C., Hobza, P., Spiegelman, F., David, F. Eds.; Les Houches, France, July 2−28, 2000, EDP Sciences and Springer Verlag: Berlin, New York, London, Paris, Tokyo, 2001.

(3) de Heer, W. A. *Rev. Mod. Phys.* **1993**, *65*, 611.

(4) *Clusters of Atoms and Molecules, Theory, Experiment and Clusters of Atoms*; Haberland, H., Ed.; Springer Series in Chemical Physics, Springer: Berlin, Heidelberg, New York, 1994; Vol. 52.

(5) *Metal Clusters*; Ekardt, W., Ed.; Wiley: New York, 1999; pp 29−68.

(6) Koopmans, T. *Physica* **1933**, *1*, 104.

(7) Cederbaum, L. S.; Schirmer, J.; Domcke, W.; von Niesse, W. *Int. Quantum Chem.* **1978**, *14*, 593.

(8) Cederbaum, L. S. *J. Phys. B* **1975**, *8*, 290.

(9) von Niessen, W.; Shirmer, J.; Cederbaum, L. S. *Comput. Phys. Rep.* **1984**, *1*, 57.

(10) Zakrzewski, V. G.; Ortiz, J. V. *Int. J. Quantum Chem., Quantum Chem. Symp.* **1994**, *28*, 23.

(11) (a) Zakrzewski, V. G.; Ortiz, J. V. *Int. J. Quantum Chem.* **1995**, *53*, 583. (b) Ortiz, J. V. *Int. J. Quantum Chem., Quantum Chem. Symp.* **1989**, *23*, 321. (c) Lin, J. S.; Ortiz, J. V. *Chem. Phys. Lett.* **1990**, *171*, 197.

(12) (a) Zakrzewski, V. G.; Ortiz, J. V.; Nichols, J. A.; Heryadi, D.; Yeager, D. L.; Golab, J. T. *Int. J. Quantum Chem.* **1996**, *60*, 29. (b) Ortiz, J. V. *Adv. Quantum Chem.* **1999**, *35*, 33.

(13) Ortiz, J. V. *J. Chem. Phys.* **1996**, *104*, 7599.

(14) Ortiz, J. V.; Zakrzewski, V. G.; Dolgounitcheva, O. In *Conceptual Trends in Quantum Chemistry*; Kryachko, E. S., Ed.; Kluwer: Dordrecht, 1997; Vol. 3, p 465.

(15) Holmes, D. L. *Elements of Physical Geology*; Ronald Press: New York, 1969; Chapter *3*.

(16) Morey, G. W. *The Properties of Glass*, 2nd ed.; Reinhold: New York, 1954; Chapter *1*.

(17) Desurvire, E. *Phys. Today* **1994**, *47*, 20.

(18) Wang, N.; Tang, Y. H.; Zhang, Y. F.; Lee, C. S.; Lee, S. T. *Phys. Rev. B* **1998**, *58*, R16024.

(19) Anderson, J. S.; Ogden, J. S. *J. Chem. Phys.* **1969**, *51*, 4189.

(20) Wang, L. S.; Nicholas, J. B.; Dupuis, M.; Wu, H.; Colson, S. D. *Phys. Rev. Lett.* **1997**, *78*, 4450.

(21) Wang, L. S.; Desai, S. R.; Wu, H.; Nicholas, J. B. Z. *Phys. D* **1997**, *40*, 36.

(22) Wang, L. S.; Wu, H.; Desai, S. R.; Fan, J.; Colson, S. D. *J. Phys. Chem.* **1996**, *100*, 8697.

(23) Chelikowsky, J. R. *Phys. Rev. B* **1998**, *57*, 3333.

(24) Snyder, L. C.; Raghavachari, K. J. *J. Chem. Phys.* **1984**, *80*, 5076.

(25) Zhang, R. Q.; Chu, T. S.; Cheung, H. F.; Wang, N.; Lee, S. T. *Phys. Rev. B* **2001**, *64*, 113304.

(26) Song, J.; Choi, M. *Phys. Rev. B* **2002**, *65*, 241302 R.

(27) Nayak, S. K.; Rao, B. K.; Jena, P. *J. Chem. Phys.* **1998**, *109*, 1245.

(28) Chu, T. S.; Zhang, R. Q.; Cheung, H. F. *J. Chem. Phys.* **2001**, *105*, 1705.

(29) Caputo, M. C.; Oña, O. B.; Ferraro, M. B. *J. Chem. Phys.* **2009**, *130*, 134115.

(30) Zang, Q. J.; Su, Z. M.; Lu, W. C.; Wang, C. Z.; Ho, K. M. *J. Phys. Chem. A* **2006**, *110*, 8151.

(31) Becke, A. D. *J. Chem. Phys.* **1993**, *98*, 5648.

(32) McLean, A. D.; Chandler, G. S. *J. Chem. Phys.* **1980**, *72*, 5639.

(33) Krishnan, B. R.; Binkley, J. S.; Seeger, R.; Pople, J. A. *J. Chem. Phys.* **1980**, *72*, 650.

(34) Ortiz, J. V. In *Computational Chemistry: Reviews of Current Trends*; Leszczynski, J., Ed.; World Scientific: Singapore, 1997; Vol. 2, p 1.

(35) Igel-Mann, G.; Stoll, H.; Preuss, H. *Mol. Phys.* **1988**, *65*, 1321.

(36) Sadlej, A. J. *Collect. Czech. Chem. Commun.* **1998**, *53*, 1995.

(37) Tiznado, W. A.; Fuentealba, P.; Ortiz, J. V. *J. Chem. Phys.* **2005**, *123*, 144314.

(38) Yang, W.; Mortier, W. J. *J. Am. Chem. Soc.* **1986**, *108*, 5708.

(39) Reed, A. E.; Curtiss, L. A.; Weinhold, F. Intermolecular Interactions from a Natural Bond Orbital, Donor-Acceptor Viewpoint. *Chem. Rev.* **1988**, *88* (6), 899–926.

(40) Reed, A. E.; Weinstock, R. B.; Weinhold, F. Natural-Population Analysis. *J. Chem. Phys.* **1985**, *83* (2), 735–746.

(41) Reed, A. E.; Weinhold, F. Natural Bond Orbital Analysis of Near-Hartree-Fock Water Dimer. *J. Chem. Phys.* **1983**, *78* (6), 4066–4073.

(42) Breneman, C. M.; Wiberg, K. B. Determining Atom-Centered Monopoles from Molecular Electrostatic Potentials - The Need for High Sampling Density in Formamide Conformational-Analysis. *J. Comput. Chem.* **1990**, *11* (3), 361–373.

(43) Frisch, M. J.; Trucks, G. W.; Schlegel, H. B.; Scuseria, G. E.; Robb, M. A.; Cheeseman, J. R.; Montgomery, J. A., Jr.; Vreven, T.; Kudin, K. N.; Burant, J. C.; Millam, J. M.; Iyengar, S. S.; Tomasi, J.; Barone, V.; Mennucci, B.; Cossi, M.; Scalmani, G.; Rega, N.; Petersson, G. A.; Nakatsuji, H.; Hada, M.; Ehara, M.; Toyota, K.; Fukuda, R.; Hasegawa, J.; Ishida, M.; Nakajima, T.; Honda, Y.; Kitao, O.; Nakai, H.; Klene, M.; Li, X.; Knox, J. E.; Hratchian, H. P.; Cross, J. B.; Bakken, V.; Adamo, C.; Jaramillo, J.; Gomperts, R.; Stratmann, R. E.; Yazyev, O.; Austin, A. J.; Cammi, R.; Pomelli, C.; Ochterski, J. W.; Ayala, P. Y.; Morokuma, K.; Voth, G. A.; Salvador, P.; Dannenberg, J. J.; Zakrzewski, V. G.; Dapprich, S.; Daniels, A. D.; Strain, M. C.; Farkas, O.; Malick, D. K.; Rabuck, A. D.; Raghavachari, K.; Foresman, J. B.; Ortiz, J. V.; Cui, Q.; Baboul, A. G.; Clifford, S.; Cioslowski, J.; Stefanov, B. B.; Liu, G.; Liashenko, A.; Piskorz, P.; Komaromi, I.; Martin, R. L.; Fox, D. J.; Keith, T.; Al-Laham, M. A.; Peng, C. Y.; Nanayakkara, A.; Challacombe, M.; Gill, P. M. W.; Johnson, B.; Chen, W.; Wong, M. W.; Gonzalez, C.; Pople, J. A. *Gaussian 03, revision E.01*; Gaussian, Inc.: Wallington, CT, 2004.

(44) Flükiger, P.; Lüthi, H. P.; Portmann, S.; Weber, J. Swiss National Supercomputing Centre CSCS, Manno, Switzerland, 2000.

(45) Dunning, T. H., Jr. *J. Chem. Phys.* **1989**, *90*, 1007.

(46) Woon, D. E.; Dunning, T. H., Jr. *Chem. Phys.* **1993**, *98*, 1358.

(47) Wang, H.; Sun, J.; Lu, W. C.; Sun, C. C.; Wang, C. Z.; Ho, K. M. *J. Phys. Chem. C* **2008**, *112*, 7097.

(48) Tiznado, W.; Oña, O. B.; Bazterra, V. E.; et al. *J. Chem. Phys.* **2005**, *123*, 214302.

CT900320R